

JMJD3 deficiency alleviates lipopolysaccharide-induced acute lung injury by inhibiting alveolar epithelial ferroptosis in a Nrf2-dependent manner

JUNWEI PENG, BIN FAN, CHUANMING BAO and CHEN JING

Department of Cardiothoracic Surgery, Suizhou Hospital,
Hubei University of Medicine, Suizhou, Hubei 441300, P.R. China

Received May 7, 2021; Accepted August 23, 2021

DOI: 10.3892/mmr.2021.12447

Abstract. Acute respiratory distress syndrome (ARDS) is a deadly illness which presents with severe hypoxemia as well as diffuse alveolar damage. Jumonji domain-containing 3 (JMJD3), which belongs to the UTX/UTY JmjC-domain protein subfamily, is involved in infection, development, aging and immune disorders. However, the role of JMJD3 in acute lung injury (ALI) is still unclear. The present study explored the roles and potential mechanisms of JMJD3 in ALI. Alveolar epithelial cell-specific knockout of JMJD3 mice and A549 alveolar epithelial cells were used to investigate the function of JMJD3 in ALI. Lipopolysaccharide (LPS) was used to establish an *in vivo* and *in vitro* ALI model. The expression of JMJD3 in murine lung tissue and alveolar epithelial cells was detected. Pathological injury of lung tissue and alveolar epithelial cells was also investigated following inhibition of JMJD3. The results showed that JMJD3 expression was significantly increased in murine lung tissues and in A549 cells following LPS stimulation. JMJD3-deficient mice in alveolar epithelial cells exhibited alleviated lung pathological injury and ferroptosis following h stimulation. Mechanistically, it was found that JMJD3 knockout could increase the expression of nuclear factor erythroid-2-related factor-2 (Nrf2) in lung tissues challenged with h. However, Nrf2 overexpression by adenovirus could further enhance the anti-ferroptotic effect from JMJD3 silence in h-treated A549 cells. Taken together, the present study revealed that JMJD3 deficiency may relieve LPS-induced ALI by blocking alveolar epithelial ferroptosis in a Nrf2-dependent manner, which may serve as a novel therapeutic target against ALI.

Introduction

Acute lung injury (ALI) is a life-threatening disease which presents with activated inflammatory response, increased penetrability of the alveoli and pulmonary edema, which can deteriorate into acute respiratory distress syndrome (ARDS) and even mortality unless it is promptly controlled (1,2). Infection and sepsis serve as critical causes contributing to ALI, as well as ischemia reperfusion, trauma and drug toxicity (3). The annual mortality for ARDS and ALI remains high worldwide, leading to a significant health-care burden although significant achievements have been made in the therapeutic strategy for ARDS and ALI (4). Alveolar epithelial cells act as the primary host defense of the alveolus, forming a robust barrier against various insult including infectious and noninfectious factors in the pathogenesis of ALI (5,6). Hence, maintaining the normal function of alveolar epithelial cells is of great importance to retard the progression of ALI.

Ferroptosis is a recently discovered form of cell death, first defined in 2012 and characterized by excessive iron accumulation as well as lipid peroxidation (7). Ferroptosis is an iron-dependent death, which differs from other regulated cell death (RCD) including apoptosis, pyroptosis, necroptosis and autophagic death (8). Recent studies have revealed that ferrostatin-1, a typical ferroptosis inhibitor, can effectively relieve lipopolysaccharide (LPS)-induced ALI in mice and human bronchial epithelial cell, indicating that ferroptosis is involved in sepsis-induced ALI (9-11). Additionally, in ALI caused by other pathogenesis including ischemia reperfusion (12), seawater drowning (13) and acute radiation (14), alveolar epithelial ferroptosis also participates in the development of ferroptosis. Nuclear factor E2 related factor 2 (Nrf2) is the core transcription factor essential for cells to keep redox homeostasis in the context of high oxidative stress (15). Nrf2 transcriptionally activates numerous anti-ferroptotic genes by binding to certain antioxidant response element in the nucleus, helping to maintain cellular survival (16). During ALI, Nrf2 blocks alveolar epithelial ferroptosis and prevents lung injury by upregulating solute carrier family 7, membrane 11 (SLC7A11) and heme oxygenase 1 (10). Based on these studies, genes or exogenous drugs that could activate Nrf2 in alveolar

Correspondence to: Professor Bin Fan, Department of Cardiothoracic Surgery, Suizhou Hospital, Hubei University of Medicine, 60 Longmen Street, Suizhou, Hubei 441300, P.R. China
E-mail: 3552356146@qq.com

Key words: Jumonji domain-containing 3, lipopolysaccharide, acute lung injury, ferroptosis, Nrf2

epithelial cells may possess the potential to inhibit ferroptosis and combat ALI.

Jumonji domain-containing 3 (JMJD3) is a histone demethylase which specifically demethylates trimethylated H3 lysine 27 (17). In the context of pathological stimulus, cytoplasm JMJD3 can be recruited around the chromatin and interact with certain transcription factors, activating the transcription of inflammatory genes, oncogenes, developmental genes and oxidative genes (17,18). A previous study showed that JMJD3 promoted the activation of Nod-like receptor family pyrin domain-containing 3 inflammasome and exacerbated colitis in mice by regulating Nrf2 (19). Upregulation of JMJD3 can give rise to the removal of the repressive histone methylation mark on NF κ B-mediated inflammatory gene promoters, thus triggering macrophage-mediated inflammation (20). These studies suggest that JMJD3 also serves a critical role in inflammatory response. However, the potential roles of JMJD3 in ALI have not been reported. The present study first investigated the expression levels of JMJD3 in sepsis-induced mice and LPS-treated A549 cells. Next, the potential roles of JMJD3 in modulating ALI were observed by using alveolar epithelial cell-specific knockout of JMJD3 mice. Finally, the possible mechanisms contributing to the protection of JMJD3 silencing were explored. The present study revealed that the expression of JMJD3 significantly increased during ALI. Alveolar epithelial cell-specific knockout of JMJD3 clearly ameliorated sepsis-induced lung injury and ferroptosis. In addition, Nrf2 overexpression further strengthen the anti-ferroptotic effect from JMJD3 silence. The findings suggested that JMJD3 functions as a possible target against ALI.

Materials and methods

Reagents. Anti-GAPDH (cat. no. ab8245), anti-NRF2 (cat. no. ab62352), anti-JMJD3 (cat. no. ab169197), anti-STA1 (cat. no. ab105220), anti-glutathione peroxidase 4 (GPX4; cat. no. ab125066), anti-prostaglandin-endoperoxide synthase 2 (PTGS2; cat. no. ab179800) and anti-SLC7A11 (cat. no. ab175186) antibodies were obtained from Abcam. Fetal bovine serum (FBS), trypsin-EDTA (0.25%) phenol red and Dulbecco's modified Eagle's medium, Nutrient Mixture F-12 (DMEM/F-12) were purchased from Gibco (Thermo Fisher Scientific, Inc.). The peroxidase-conjugated secondary antibody was obtained from LI-COR Biosciences. The QuantiPro Bicinchoninic Acid Protein Assay kit from Sigma-Aldrich (Merck KGaA) was employed to detect protein concentrations. All chemical reagents used in the present study were of analytical grade.

Animals and animal models. All procedures in this study were in accordance with the Guide for the Care and Use of Laboratory Animals of National Institutes of Health for live animals (21). All animal experiments were approved by the Ethics Committee of the Wuhan University (approval no. YXLL-2020-102). A total of 30 male C57/B6J mice (8-10 weeks, 21-23 g) were acquired from Chinese Academy of Medical Sciences (Beijing, China). A total of 16 Jmjd3-flox mice and five Sftpc-cre⁺ mice with C57/B6J background were provided by Model Animal Research Center of Nanjing

University. The surfactant protein C (SPC) is exclusively expressed in the type II alveolar epithelial cells. Sftpc-cre; 25 male Jmjd3^{+/flox} mice (genotype Sftpc-cre^{+/+}; Jmjd3^{+/flox}; age, 8-10 weeks; weight, 20-24 g) were generated through breeding Jmjd3^{flox/flox} mice and Sftpc-cre^{+/+} mice. All animals housed under specific pathogen-free conditions in a humidity-(40-60%)-and temperature (18-25°C)-controlled environment with a 12-h light/dark cycle and free access to water and food. JMJD3 expression was detected via western blotting. In subsequent experiments, male mice as well as their wild-type littermates (8-10 weeks, 21-23 g) were used. The sepsis-induced ALI model was constructed by administering LPS intratracheally (5 mg/kg) for 12 h as previously reported (22). The control groups were given an isovolumetric sterile saline. Then, 12 h after LPS installation, the animals were sacrificed by cervical dislocation under deep anesthesia with an intraperitoneal injection of 2% sodium pentobarbital (60 mg/kg). Next, the left lungs from 5 mice from each group were excised and placed in formalin (10%) for 3 days to expand the alveoli at room temperature. The left lungs from the other 5 mice in each group were dried in an 80°C oven for 3 days. The lung wet/dry (W/D) ratio was calculated to assess edema. The right lung tissues were stored at -80°C for biochemical analysis.

Cell culture and treatment. A549 alveolar epithelial cells were purchased from Kunming Cell Bank of Typical Cultures Preservation Committee, Chinese Academy of Sciences (Kunming, China). The A549 alveolar epithelial cells were incubated at 37°C with DMEM supplemented with 10% FBS in a 5% CO₂ incubator. JMJD3 small interfering RNA (siRNA) and the negative control were obtained from Shanghai GenePharma Co. Ltd. The primers were as follows: JMJD3 forward, 5'-GACACUATCTACTAACTATACTTA-3' and reverse, 5'-CCCUAGCTAGTCUUUAAACC-3' and negative control forward, 5'-CACATGCTGATGCTAUCTU-3' and reverse, 5'-ACUTTCTATCUTACTACAA-3'.

The epithelial cells were transfected using Lipofectamine[®] 3000 (Invitrogen; Thermo Fisher Scientific, Inc.) and siRNA (50 nmol/m) based on the manufacturer's instructions at room temperature for 20 h. Subsequently, to mimic sepsis-induced lung injury, the A549 alveolar epithelial cells were treated with LPS at the concentration of 100 ng/ml with Ad-Nrf2 (MOI=25) or adenovirus harboring no overexpression sequence (Ad-vector) for 6 h. Based on a previous study (23), mouse AT2 cells in Jmjd3^{flox/flox} mice and Sftpc-cre; Jmjd3^{+/flox} mice were isolated. In brief, mice were perfused with phosphate buffer solution and then injected with 0.5 ml 1% low-melting agarose and 2 ml dispase into lung lobe. Then the lung tissue was incubated with AT2 isolation medium supplemented with 0.01% DNase I after removing trachea and airways for 0.5 h at 37°C. The mixture was subsequently filtered and re-suspended with AT2 isolation medium containing a 1:1 mixture of DMEM/F-12 supplemented with 10% FBS, 100 U/ml sodium penicillin G, and 100 μ g/ml streptomycin for 1 h. Cells were centrifuged for 10 min at 4°C at 300 x g and incubated on pre-coated dishes with mouse IgG at 4°C. After 2 h, non-adherent cells were collected, centrifuged for 5 min at 4°C at 200 x g and re-suspended with AT2 isolation medium.

Table I. Primers.

Species	Gene	Forward primer	Reverse primer
Human	<i>SLC7A11</i>	CGTAGCTGTGATAGTAGCTG	CAGTCGTATAGTCGTGATCCCC
Human	<i>GPX4</i>	AGCTAGTGAATATGCTGTACCC	CGATAGATGCTGTAGCTGATGCC
Human	<i>JMJD3</i>	CGATCGTAGTAGATCGTAGTC	CGATGCTGATGCTGATGCTGAA
Human	<i>GAPDH</i>	CGATGTCGATAGTGCTAGTCA	CAGGCTGATCGTAGTCGTGAGCTA
Mice	<i>JMJD3</i>	CGATGCTGATGTCGTAGTCGTA	CAGCTAGTGCTCGTAGTCGTGATC
Mice	<i>GAPDH</i>	AACAGTCGTAGTCGTAGATGTT	CAGTCGTAGTCGTAGTCGTATAAC

SLC7A11, solute carrier family 7, membrane 11; *GPX4*, glutathione peroxidase 4; *JMJD3*, Jumonji domain-containing 3.

Hematoxylin and eosin (H&E) and immunofluorescence staining. To evaluate the LPS-induced lung injury model and therapeutic potential of JMJD3, the left lungs were removed from mice in each group and subsequently fixed in 4% formalin overnight at room temperature. Lung tissue samples were dehydrated in ascending ethanol series and embedded in paraffin. After the paraffin blocks were cut into 3 μ m-thick sections, they were fixed in ethanol as follows: Immersed in 70, 80 and 90% ethanol for 4-5 sec, then immersed in anhydrous ethanol for 5 min at room temperature. Subsequently, hematoxylin staining was performed for 5 min and eosin staining was performed for 1 min at room temperature to assess morphological abnormalities and inflammation score in a blinded fashion as described previously (22). In brief, the severity of the lung injury was graded from 0 to 4, on the basis of five independent variables: Neutrophils in the alveolar space, hemorrhage, pertinacious debris filling the airspaces, hyaline membranes, and septal thickening. Scoring was as follows: 4, >75; 3, 51-75; 2, 25-50; 1, <25 and 0, 0% damage.

To observe the protein expression of JMJD3, immunofluorescence staining was performed based on previous study (24). In brief, the medium in the 24-well plate containing A549 alveolar epithelial cells was discarded, following by fixation with 4% paraformaldehyde at room temperature for 5 min. Then 0.1% Triton X-100 was used to permeabilize cells. Cells were incubated with primary JMJD3 antibody (1:200) overnight at 4°C; fluorescein isothiocyanate-conjugated goat anti-rabbit IgG (1:300) was added to incubate for 1 h at 37°C away from light. Sections were incubated with DAPI to stain the nuclei at room temperature. The protein expression of JMJD3 was observed under an immunofluorescence microscope (magnification, x400).

Detection of bronchoalveolar lavage fluid (BALF). The BALF was acquired via intratracheal injections of 1.0 ml of cooled phosphate buffer saline (PSB) three times after the mice were sacrificed. Then the BALF was centrifuged at 1,200 x g for 10 min at 4°C. Total cells, macrophages and neutrophil were calculated using a hemocytometer as well as Wright-Giemsa staining as described previously (25). In brief, a drop of BALF was placed onto a slide to make a smear. Smears were air dried and then fixed in methanol (100%) for 3 min at room temperature. Slides were stained with Wright-Giemsa working solution for 1 min at room temperature and subsequently visualized using a light microscope (magnification, x400).

Reverse transcription-quantitative (RT-q) PCR. Total RNA was extracted from the A549 alveolar epithelial cells (3×10^6) using the Transcriptor First Strand cDNA Synthesis kit (Norgen) according to the protocol. RNA concentration was detected using a Biodrop μ liTe Pc spectrophotometer. Then the total RNA was synthesized into cDNA using Prime Script RT Master Mix; the RT reaction conditions were 37°C for 15 min, followed by 85°C for 5 sec. PCR was performed using the LightCycler 480 SYBR Green 1 Master Mix (Roche Diagnostics GmbH). The thermocycling conditions were as follows: Denaturation for 10 sec at 95°C, 20 sec annealing at 60°C and final extension for 20 sec at 72°C. All primers used in this study are given in Table I. The mRNA levels were calculated with the $2^{-\Delta\Delta Cq}$ method and normalized to GAPDH (26).

Western blot analysis. Total proteins in iced cell lysates and right lung tissues were extracted after cells and tissues were lysed by a RIPA buffer. The protein concentrations were then measured using a commercial BCA Protein Assay kit. Subsequently, the total proteins (80-100 g) were loaded into 10% SDS-PAGE gel, which were next transferred on a PVDF membrane. After blocking with milk (5%) for 1 h at room temperature, the membranes were incubated with JMJD3 (cat. no. ab169197, 1:500, Abcam.), GAPDH (cat. no. ab8245, 1:1,000, Abcam.), PTGS2 (cat. no. ab179800, 1:1,000, Abcam.), SAT1 (cat. no. ab105220, 1:1,000, Abcam), GPX4 (cat. no. ab125066, 1:1,000, Abcam), SLC7A11 (cat. no. ab175186, 1:200, Abcam) and NRF2 (cat. no. ab62352, 1:500, Abcam) overnight at 4°C and peroxidase-conjugated goat anti-rabbit IgG (cat. no. SA00001-2; 1:5,000; ProteinTech Group, Inc.) for 2 h at room temperature. Finally, the membranes were screened and visualized via an Odyssey Imaging System (LI-COR Biosciences). Blots were quantitated using Image Lab software 4.0 (Bio-Rad Laboratories, Inc.). The protein levels in this study were normalized to GAPDH.

Statistical analysis. The data are presented as mean \pm standard error of mean and were analyzed by SPSS 23.0 (IBM Corp.). Comparisons between two groups were performed by Student's unpaired t-test. Multiple comparisons among ≥ 3 groups were performed by one-way ANOVA, followed by post hoc Tukey's test. $P < 0.05$ was considered to indicate a statistically significant difference.

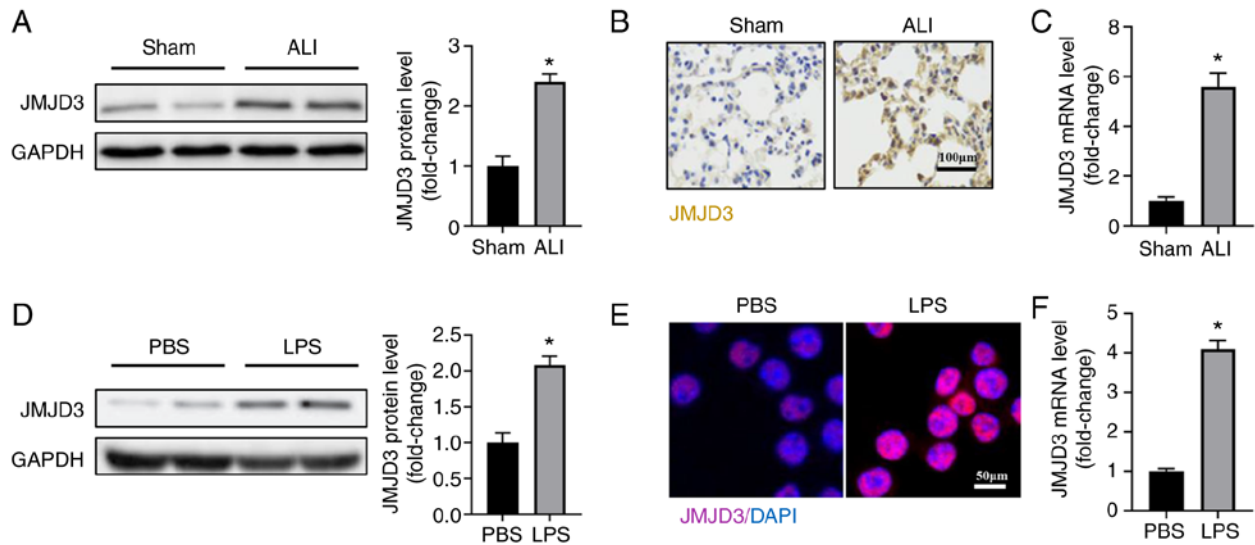


Figure 1. The expression of JMJD3 in LPS-treated lung tissues and alveolar epithelial cells. (A) Western blotting and statistical results for JMJD3 in lung tissues. (B) Immunohistochemistry staining for JMJD3 protein in lung tissues. (C) The mRNA level of JMJD3 in lung tissues (n=5; *P<0.05 vs. Sham group). (D) Western blotting and statistical results for JMJD3 in alveolar epithelial cells. (E) Immunofluorescent staining for JMJD3 protein in alveolar epithelial cells. (F) The mRNA level of JMJD3 in lung tissues (n=5; *P<0.05 vs. PBS group). JMJD3, Jumonji domain-containing 3; LPS, lipopolysaccharide; ALI, acute lung injury.

Results

The expression of JMJD3 in LPS-treated lung tissues and alveolar epithelial cells. To explore the association between JMJD3 and sepsis-induced ALL, the protein and mRNA levels of JMJD3 were detected in a murine model of ALI. As shown in Fig. 1A–C, the protein and mRNA levels of JMJD3 were significantly upregulated in mice with ALI compared with control group. LPS stimulation also increased the protein and mRNA levels of JMJD3 in A549 alveolar epithelial cells (Fig. 1D–F). It was also found that JMJD3 mainly expressed in nucleus of alveolar epithelial cells. Taken together, these data showed that the expression of JMJD3 was upregulated in response to LPS stimulation.

JMJD3 deficiency relieved LPS-induced ALI. To understand the effect of JMJD3 on LPS-induced ALI, alveolar epithelial cell-specific knockout of *Jmjd3* mice (JMJD3-CKO) was constructed. Alveolar epithelial cell-specific deletion of JMJD3 was verified by western blotting (Fig. 2A). H&E staining (Fig. 2B) showed that mice challenged with LPS developed marked lung injury, as evidenced by thickening of alveolar walls, lung edema, alveolar hemorrhage and a higher inflammation score. The lung wet/dry ratio and cells count including total cell, macrophage and neutrophil in BALF were significantly higher in ALI-Flox group than those in Sham-Flox group (Fig. 2C–F). However, JMJD3 knockout significantly alleviated LPS-induced lung edema and infiltration of inflammatory cells in BALF. Collectively, these data demonstrated that JMJD3 deficiency contributed to the improvement of LPS-induced ALI.

JMJD3 deficiency inhibited ferroptosis in LPS-treated lung. Alveolar epithelial ferroptosis could aggravate ALI induced by LPS. The protein markers of ferroptosis in were next detected the indicated four groups. As shown in Fig. 3, LPS stimulation significantly increased the protein levels of PTGS2 and

SAT1 and decreased the protein levels of GPX4 and SLC7A11, indicating that LPS triggered ferroptosis in lung. Compared with the ALI-Flox group, the mice in ALI-CKO group displayed lower level of ferroptosis, which was evidenced by the decreased levels of PTGS2 and SAT1 and higher levels of GPX4 as well as SLC7A11. These results hinted that alveolar epithelial cell-specific knockout of JMJD3 could repress the level of ferroptosis induced by LPS.

Nrf2 is involved in the protection of JMJD3 deficiency in vivo and in vitro. Previous studies have illustrated that Nrf2 could transcriptionally activate certain anti-ferroptotic genes including Gpx4 and Slc7a11 (16,27). Meanwhile, the expression of Nrf2 could be also modulated by JMJD3 (19). Therefore, the protein level of Nrf2 was detected in the 4 groups. The results (Fig. 4A) showed that alveolar epithelial cell-specific knockout of JMJD3 inhibited the decrease of Nrf2 in lung tissues challenged with LPS. To further verify the relationship between Nrf2 and JMJD3, Nrf2 was overexpressed using adenovirus and the level of JMJD3 inhibited using siRNA in A549 alveolar epithelial cells. Fig. 4B showed that the expression of JMJD3 protein was significantly inhibited following JMJD3 siRNA treatment while the expression of Nrf2 protein was significantly upregulated after transfection with Ad-Nrf2. As shown in Fig. 4C and D, JMJD3 inhibition significantly increased the mRNA levels of Slc7a11 and Gpx4 in alveolar epithelial cells, the effect of which could be enhanced after Nrf2 was overexpressed. These data suggested that JMJD3 inhibition could decrease alveolar epithelial ferroptosis in a Nrf2-dependent manner.

Discussion

The present study found that LPS stimulation led to lung injury and inflammatory response by triggering alveolar epithelial ferroptosis and alveolar epithelial cell-specific knockout of

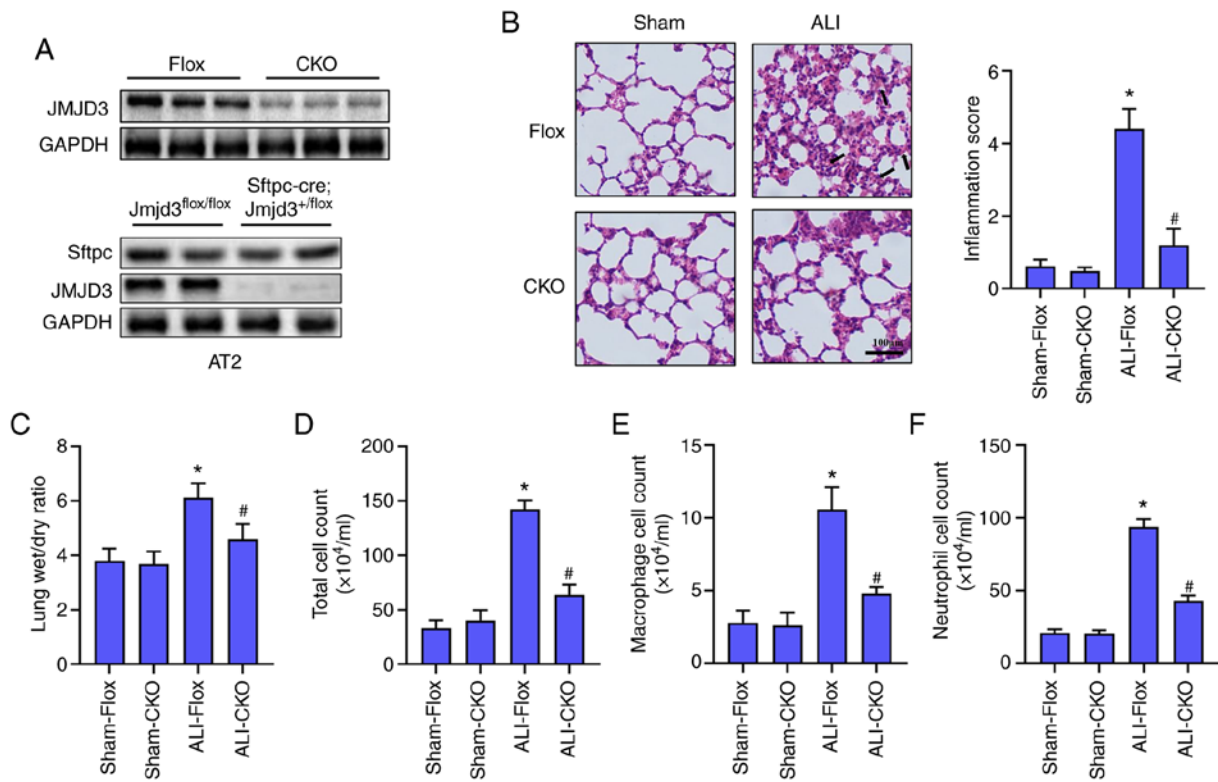


Figure 2. JMJD3 deficiency relieves LPS-induced ALI. (A) Representative blots of JMJD3 expression in lung tissues and AT2 in the indicated groups. (B) Hematoxylin and eosin staining and inflammation score of lung tissues. (C) Lung wet/dry ratio in the indicated groups. (D-F) Inflammatory cells count in BALF in the indicated groups (n=5; *P<0.05 vs. Sham-Flox group; #P<0.05 vs. ALI-Flox group). JMJD3, Jumonji domain-containing 3; LPS, lipopolysaccharide; ALI, acute lung injury; BALF, bronchoalveolar lavage fluid.

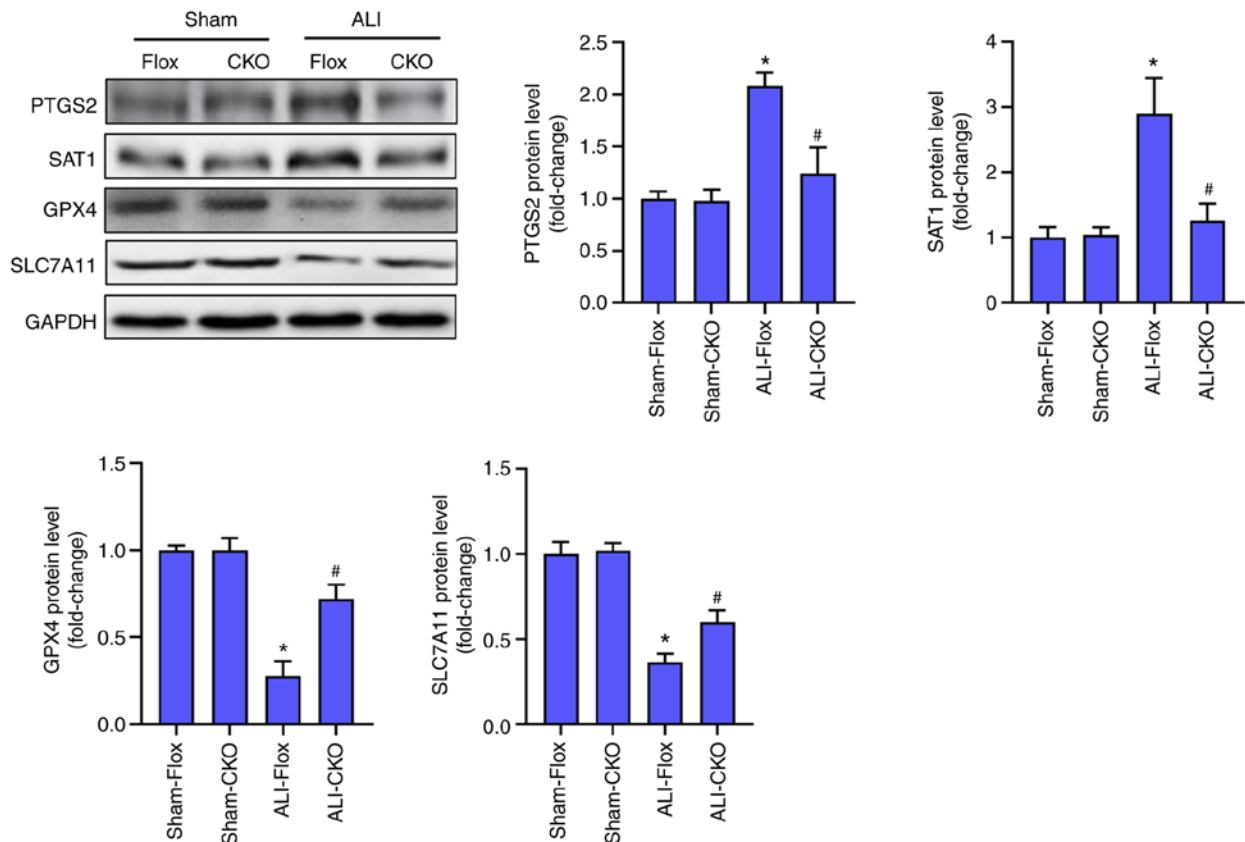


Figure 3. JMJD3 deficiency inhibits ferroptosis in LPS-treated lung. Western blotting and statistical results for PTGS2, SAT1, GPX4 and SLC7A11 in lung tissues (n=5; *P<0.05 vs. Sham-Flox group; #P<0.05 vs. ALI-Flox group). JMJD3, Jumonji domain-containing 3; LPS, lipopolysaccharide; PTGS2, prostaglandin-endoperoxide synthase 2; GPX4, glutathione peroxidase 4; SLC7A11, solute carrier family 7, membrane 11.

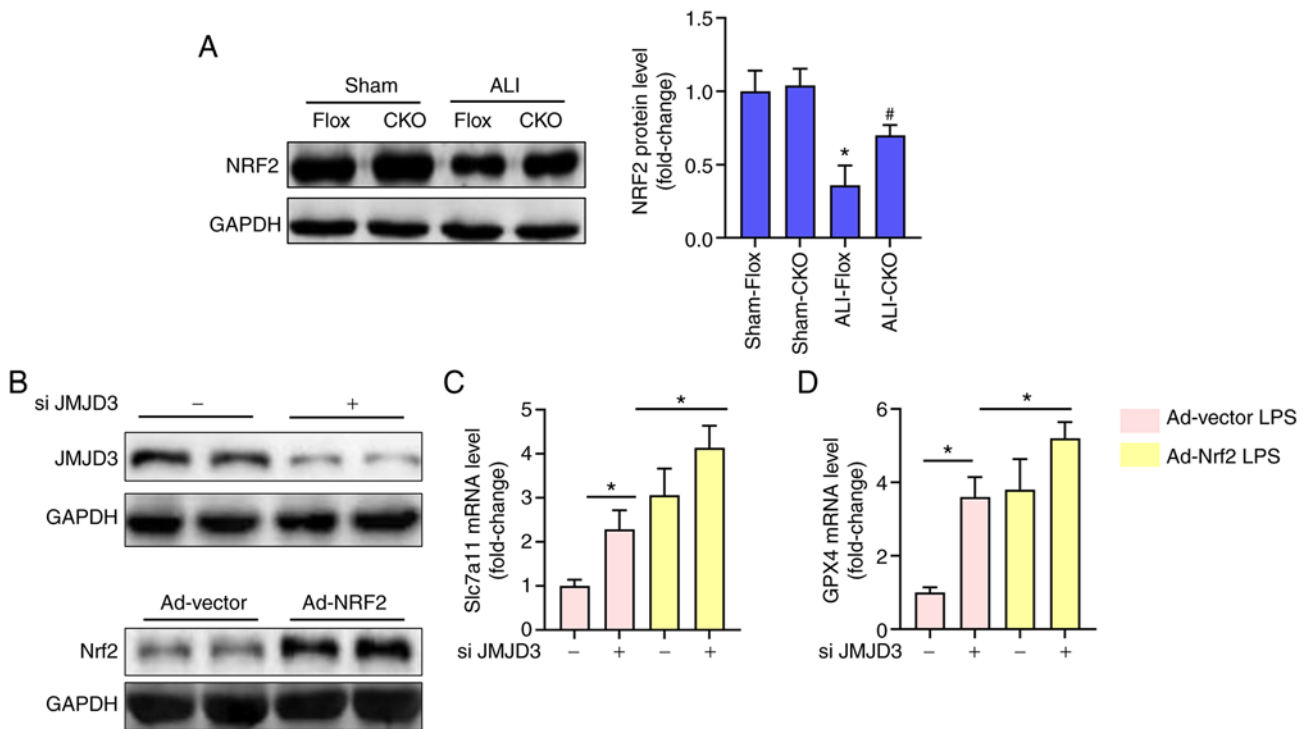


Figure 4. Nrf2 is involved in the protection of JMJD3 deficiency *in vivo* and *in vitro*. (A) Western blotting and statistical results for Nrf2 in lung tissues in the indicated groups (n=5; *P<0.05 vs. Sham-Flox group; #P<0.05 vs. ALI-Flox group). (B) Representative blot of JMJD3 expression and Nrf2 expression in A549 alveolar epithelial cells treated with JMJD3 siRNA. The mRNA levels of (C) SLC7A11 and (D) GPX4 in A549 alveolar epithelial cells in the indicated groups (n=5 samples; *P<0.05 vs. indicated group). Nrf2, nuclear factor erythroid-2-related factor-2; JMJD3, Jumonji domain-containing 3; ALI, acute lung injury; siRNA, small interfering RNA; GPX4, glutathione peroxidase 4; SLC7A11, solute carrier family 7, membrane 11

JMJD3 significantly alleviated lung injury caused by sepsis through blocking ferroptosis. Mechanistically, JMJD3 deficiency could reverse the decrease of Nrf2 during ALI, hence increasing the transcription levels of anti-ferroptotic genes including GPX4 and SLC7A11. Based on these findings, it was hypothesized that JMJD3 may serve as a potential target against sepsis-induced ALI.

Cells can die from accidental cell death (such as necrosis) and RCD (such as pyroptosis, ferroptosis, apoptosis, necroptosis and autophagy), of which ferroptosis is closely involved in infection and solid organ injury (28,29). Initiation of ferroptosis demands three critical foundations including abundant redox-active iron in cytoplasm, vital substrates undergoing peroxidation and the failure of the lipid peroxide repair network. SLC7A11 is one of the subunits of system Xc⁻, which is in essence a cystine/glutamate reverse transporter. SLC7A11 is mainly expressed on cell membrane and responsible for cystine import, which is important for maintaining cellular redox homeostasis. The intracellular cystine could be degraded to cysteine, which is then synthesized into antioxidant GSH (16,30).

As with system Xc⁻, GPX4 can also negatively regulate ferroptosis via exerting antioxidant effects (31). In detail, GPX4 can convert reduced glutathione to oxidized glutathione through reducing lipid hydroperoxides to lipid hydroxy derivative or converting free hydrogen peroxide to water, maintaining the redox homeostasis in cell (16). A number of studies have reported that ferroptosis is involved in the development of lung injury. For instance, Liu *et al* (9) reported that LPS treatment significantly decreases the viability of a human

bronchial epithelial cells and the levels of SLC7A11 and GPX4, which could be reversed by Ferrostatin-1. Additionally, intestinal ischemia/reperfusion-induced ALI also promotes alveolar epithelial ferroptosis, which can in turn be aggravated by erastin (32). As a basic leucine zipper transcription factor modulating the expression of antioxidant genes associated with redox homeostasis, Nrf2 can inhibit ferroptosis by regulating ferroptotic core genes indirectly, including GPX4 and SLC7A11, thus exerting protection in ALI (10,32). In parallel with these studies, the present study also revealed that Nrf2 overexpression by adenovirus could promote the protective effects of JMJD3 deficiency in LPS-treated alveolar epithelial cells.

JMJD3 is a histone demethylase which can demethylate trimethylated H3 lysine 27 (33). LPS can upregulate the expression of JMJD3 by activating NF- κ B in macrophages and vascular endothelial cells, eventually increasing the expression of inflammatory genes (34,35). Consistent with previous studies, the present study also found that LPS could increase the protein and mRNA levels of JMJD3 in murine lung tissues and alveolar epithelial cells. In addition, JMJD3 deficiency in alveolar epithelial cells not only alleviated LPS-induced lung injury and inflammatory response, but also inhibited ferroptosis in lung tissues. Furthermore, JMJD3 deficiency enhanced the protein expression of Nrf2 in murine lung tissues challenged with LPS. *In vitro* experiments also showed that Nrf2 overexpression increased the anti-ferroptotic ability of JMJD3 siRNA in alveolar epithelial cells by upregulating the expression levels of GPX4 and SLC7A11. However, there are still some limitations to the present study. For instance, the

A549 cell used is in essence a tumor cell line. Although it also possessed the characteristics of type II alveolar epithelial cells, A549 cells could not represent alveolar epithelial cells completely. Hence, future study should further explore the roles of JMJD3 in primary alveolar epithelial cells.

In summary, the present study proposed that LPS stimulation not only gave rise to lung injury by inducing alveolar epithelial ferroptosis, but also increased the level of JMJD3. JMJD3 deficiency in alveolar epithelial cells could protect against LPS-induced ALI, the potential mechanism of which involves the activation of the Nrf2 in epithelial cells. The present study for the first time, to the best of the authors' knowledge, revealed that JMJD3 deficiency may prevent the harmful effects of LPS on lung tissues, which is expected to serve as a possible candidate against lung injury caused by sepsis.

Acknowledgements

Not applicable.

Funding

The present study was supported by Scientific Research Program Guiding Project of Education Department, Hubei Province (grant no. B2017482).

Availability of data and materials

The datasets used and/or analyzed during the current study are available from the corresponding author on reasonable request.

Authors' contributions

JP and BF conceived the study and revised the manuscript. CB and CJ performed the experiments and data analysis. All authors confirm the authenticity of all the raw data. All authors have read and approved the final manuscript.

Ethics approval and consent to participate

All animal experiments were approved by the Ethics Committee of the Wuhan University (approval no. YXLL-2020-102).

Patient consent for publication

Not applicable.

Competing interests

The authors declare that they have no competing interests.

References

- Santa Cruz R, Villarejo F, Irrazabal C and Ciapponi A: High versus low positive end-expiratory pressure (PEEP) levels for mechanically ventilated adult patients with acute lung injury and acute respiratory distress syndrome. *Cochrane Database Syst Rev* 3: CD009098, 2021.
- Bian S, Cai H, Cui Y, Liu W and Xiao C: Nanomedicine-based therapeutics to combat acute lung injury. *Int J Nanomedicine* 16: 2247-2269, 2021.
- Shi J, Yu T, Song K, Du S, He S, Hu X, Li X, Li H, Dong S, Zhang Y, *et al*: Dexmedetomidine ameliorates endotoxin-induced acute lung injury in vivo and in vitro by preserving mitochondrial dynamic equilibrium through the HIF-1 α /HO-1 signaling pathway. *Redox Biol* 41: 101954, 2021.
- Fan E, Brodie D and Slutsky A: Acute respiratory distress syndrome: Advances in diagnosis and treatment. *JAMA* 319: 698-710, 2018.
- Kamio N, Hayata M, Tamura M, Tanaka H and Imai K: Porphyromonas gingivalis enhances pneumococcal adhesion to human alveolar epithelial cells by increasing expression of host platelet-activating factor receptor. *FEBS Lett* 595: 1604-1612, 2021.
- Mu M, Gao P, Yang Q, He J, Wu F, Han X, Guo S, Qian Z and Song C: Alveolar epithelial cells promote igf-1 production by alveolar macrophages through TGF- β to suppress endogenous inflammatory signals. *Front Immunol* 11: 1585, 2020.
- Geng Z, Guo Z, Guo R, Ye R, Zhu W and Yan B: Ferroptosis and traumatic brain injury. *Brain Res Bull* 172: 212-219, 2021.
- Dixon S, Lemberg K, Lamprecht M, Skouta R, Zaitsev EM, Gleason CE, Patel DN, Bauer AJ, Cantley AM, Yang WS, *et al*: Ferroptosis: An iron-dependent form of nonapoptotic cell death. *Cell* 149: 1060-1072, 2012.
- Liu P, Feng Y, Li H, Chen X, Wang G, Xu S, Li Y and Zhao L: Ferrostatin-1 alleviates lipopolysaccharide-induced acute lung injury via inhibiting ferroptosis. *Cell Mol Biol Lett* 25: 10, 2020.
- Dong H, Qiang Z, Chai D, Peng J, Xia Y, Hu R and Jiang H: Nrf2 inhibits ferroptosis and protects against acute lung injury due to intestinal ischemia reperfusion via regulating SLC7A11 and HO-1. *Aging* 12: 12943-12959, 2020.
- Xu W, Deng H, Hu S, Zhang Y, Zheng L, Liu M, Chen Y, Wei J, Yang H and Lv X: Role of ferroptosis in lung diseases. *J Inflamm Res* 14: 2079-2090, 2021.
- Xu Y, Li X, Cheng Y, Yang M and Wang R: Inhibition of ACSL4 attenuates ferroptotic damage after pulmonary ischemia-reperfusion. *FASEB J* 34: 16262-16275, 2020.
- Qiu YB, Wan BB, Liu G, Wu YX, Chen D, Lu MD, Chen JL, Yu RQ, Chen DZ and Pang QF: Nrf2 protects against seawater drowning-induced acute lung injury via inhibiting ferroptosis. *Respir Res* 21: 232, 2020.
- Li X, Zhuang X and Qiao T: Role of ferroptosis in the process of acute radiation-induced lung injury in mice. *Biochem Biophys Res Commun* 519: 240-245, 2019.
- Song M, Lee D, Chun K and Kim E: The Role of NRF2/KEAP1 signaling pathway in cancer metabolism. *Int J Mol Sci* 22: 4376, 2021.
- Li N, Jiang W, Wang W, Xiong R, Wu X and Geng Q: Ferroptosis and its emerging roles in cardiovascular diseases. *Pharmacol Res* 166: 105466, 2021.
- Zhang X, Liu L, Yuan X, Wei Y and Wei X: JMJD3 in the regulation of human diseases. *Protein Cell* 10: 864-882, 2019.
- Shentu Y, Tian Q, Yang J, Liu X, Han Y, Yang D, Zhang N, Fan X, Wang P, Ma J, *et al*: Upregulation of KDM6B contributes to lipopolysaccharide-induced anxiety-like behavior via modulation of VGLL4 in mice. *Behav Brain Res* 408: 113305, 2021.
- Huang M, Wang Q, Long F, Di Y, Wang J, Zhun Zhu Y and Liu X: Jmjd3 regulates inflammasome activation and aggravates DSS-induced colitis in mice. *FASEB J* 34: 4107-4119, 2020.
- Davis F, denDekker A, Joshi AD, Wolf SJ, Audu C, Melvin WJ, Mangum K, Riordan MO, Kunkel SL and Gallagher KA: Palmitate-TLR4 signaling regulates the histone demethylase, JMJD3, in macrophages and impairs diabetic wound healing. *Eur J Immunol* 50: 1929-1940, 2020.
- Deng W, He J, Tang XM, Li CY, Tong J, Qi D and Wang DX: Alcohol inhibits alveolar fluid clearance through the epithelial sodium channel via the A2 adenosine receptor in acute lung injury. *Mol Med Rep* 24: 725, 2021.
- Ning L, Wei W, Wenyang J, Rui X and Qing G: Cytosolic DNA-STING-NLRP3 axis is involved in murine acute lung injury induced by lipopolysaccharide. *Clin Transl Med* 10: e228, 2020.
- Do DC, Zhang Y, Tu W, Hu X, Xiao X, Chen J, Hao H, Liu Z, Li J, Huang SK, *et al*: Type II alveolar epithelial cell-specific loss of RhoA exacerbates allergic airway inflammation through SLC26A4. *JCI Insight* 6: e148147, 2021.
- Yu Y, Jiang P, Sun P, Su N and Lin F: Pulmonary coagulation and fibrinolysis abnormalities that favor fibrin deposition in the lungs of mouse antibody-mediated transfusion-related acute lung injury. *Mol Med Rep* 24: 601, 2021.

25. Huang X, Liu W, Zhou Y, Sun M, Yang HH, Zhang CY and Tang SY: Galectin-1 ameliorates lipopolysaccharide-induced acute lung injury via AMPK-Nrf2 pathway in mice. *Free Radic Biol Med* 146: 222-233, 2020.
26. Livak KJ and Schmittgen TD: Analysis of relative gene expression data using real-time quantitative PCR and the 2(-Delta Delta C(T)) method. *Methods* 25: 402-408, 2001.
27. Song X and Long D: Nrf2 and ferroptosis: A new research direction for neurodegenerative diseases. *Front Neurosci* 14: 267, 2020.
28. Li N, Wang W, Zhou H, Wu Q, Duan M, Liu C, Wu H, Deng W, Shen D and Tang Q: Ferritinophagy-mediated ferroptosis is involved in sepsis-induced cardiac injury. *Free Radic Biol Med* 160: 303-318, 2020.
29. Xu S, He Y, Lin L, Chen P, Chen M and Zhang S: The emerging role of ferroptosis in intestinal disease. *Cell Death Dis* 12: 289, 2021.
30. Wu X, Li Y, Zhang S and Zhou X: Ferroptosis as a novel therapeutic target for cardiovascular disease. *Theranostics* 11: 3052-3059, 2021.
31. Yao Y, Chen Z, Zhang H, Chen C, Zeng M, Yunis J, Wei Y, Wan Y, Wang N, Zhou M, *et al*: Selenium-GPX4 axis protects follicular helper T cells from ferroptosis. *Nat Immunol* 22: 1127-1139, 2021.
32. Li Y, Cao Y, Xiao J, Shang J, Tan Q, Ping F, Huang W, Wu F, Zhang H and Zhang X: Inhibitor of apoptosis-stimulating protein of p53 inhibits ferroptosis and alleviates intestinal ischemia/reperfusion-induced acute lung injury. *Cell Death Differ* 27: 2635-2650, 2020.
33. Liu Z, Cao W, Xu L, Chen X, Zhan Y, Yang Q, Liu S, Chen P, Jiang Y, Sun X, *et al*: The histone H3 lysine-27 demethylase Jmjd3 plays a critical role in specific regulation of Th17 cell differentiation. *J Mol Cell Biol* 7: 505-516, 2015.
34. Yu S, Chen X, Xiu M, He F, Xing J, Min D and Guo F: The regulation of Jmjd3 upon the expression of NF- κ B downstream inflammatory genes in LPS activated vascular endothelial cells. *Biochem Biophys Res Commun* 485: 62-68, 2017.
35. De Santa F, Narang V, Yap ZH, Tusi BK, Burgold T, Austenaa L, Bucci G, Caganova M, Notarbartolo S, Casola S, *et al*: Jmjd3 contributes to the control of gene expression in LPS-activated macrophages. *EMBO J* 28: 3341-3352, 2009.